

# Connectivity, clusters, and transport: use of percolation concepts and atomistic simulation to track intracellular ion migration

BY ANN MARIE SASTRY<sup>1</sup> AND CHRISTIAN M. LASTOSKIE<sup>2</sup>

<sup>1</sup>*Department of Mechanical Engineering and  
Department of Biomedical Engineering,*

<sup>2</sup>*Department of Civil and Environmental Engineering and  
Department of Biomedical Engineering, University of Michigan,  
Ann Arbor, MI 48109-2125, USA (amsastry@umich.edu)*

*Published online 31 August 2004*

The cytoskeleton is an intracellular highway system, teeming with signalling ions that zip from site to site along filaments. These tiny particles alternately embrace and slip free of protein receptors with wide-ranging affinities, as they propagate in a blur of motion along cytoskeletal corridors at transport rates far exceeding ordinary diffusive motion. Recent experimental breakthroughs have enabled optical tracking of these single ion-binding events in the physiological and diseased states. However, traditional continuum modelling methods have proven ineffective for modelling migration of biometals such as copper and zinc, whose cytosolic concentrations are putatively vanishingly small, or very tightly controlled. Rather, the key modelling problem that must be solved for biometals is determination of the optimal placement of biosensors that bind and detect the metal ions within the heterogeneous environment of the cell. We discuss herein how percolation concepts, in combination with atomistic simulation and sensor delivery models, have been used to gain insights on this problem, and a roadmap for future breakthroughs.

**Keywords:** percolation; cluster statistics; ion transport; protein binding;  
cell structure; molecular simulation

## 1. Introduction

If one could be shrunk so as to sit astride a single, fine, filamentary protein in the relatively vast, yet intricate and locally specialized, cytoskeletal structure supporting a cell (figure 1), the heterogeneity within the cytosol, and the stochastic nature of interactions of proteins and ions would be self-evident. The rapidly changing trajectories of signalling ions (e.g.  $\text{Ca}^{2+}$ ,  $\text{K}^+$ ,  $\text{Na}^+$ ) in the cell might appear alternately as Brownian flashes zinging madly among membranes and into and out of organelles, or even as organized clusters of ions into ‘blips’ or ‘puffs’, or waves, using terms describing calcium transport (Bootman *et al.* 1997).

One contribution of 17 to a Triennial Issue ‘Chemistry and life science’.

Table 1. *Several widely used forms of linear, partial differential equations used to solve problems in physics*

(Formulations, applications and solution methods are as shown.)

equation	formula	phenomena	solution
wave	$\nabla^2 U = \kappa \frac{\partial U}{\partial t}$	wave	analytical: Bäcklund transformation, Green's function; integral transformation, Lax pair, separation of variables; numerical: FEM
diffusion	$\frac{\partial U}{\partial t} = \kappa \nabla^2 U$	heat conduction, mass diffusion	analytical: separation of variables, Laplace transform, Fourier transform, Green's function; numerical: FEM
Poisson	$\nabla^2 U = 4\pi\rho$	electrostatics with constant source or sink, thermal field with constant source or sink	analytical: separation of variables, Laplace transform, Fourier transform, Green's function; numerical: FEM
Laplace	$\nabla^2 U = 0$	thermal conduction, electrostatics, incompressible fluid flow, membrane mechanics, elasticity	analytical: separation of variables, Laplace transform, Fourier transform, Green's function; numerical: FEM

Practical experimental markers for microscopic visualization of ions moving in cells require two basic elements: first, a molecule, generally a protein of many times the atomic mass of the ion, must be found to bind the ion, and second, a means of imaging that molecule in its bound configuration must be found. For the second requirement, use of fluorescent end-groups is a common approach, and sensors for ion transport in wide use, range from free dyes to discrete, bioinert nanoprobcs. Following very early work (1881–1887) by the British physiologist Sidney Ringer, who demonstrated conclusively that certain salts were essential for the proper performance of the isolated perfused frog heart—calcium ( $\text{Ca}^{2+}$ ), potassium ( $\text{K}^+$ ) and sodium ( $\text{Na}^+$ )—generations of workers have successively improved means of targeted ionic imaging.

(a) *Transport modelling: from diffusion to direct stochastic simulation*

Einstein, in one of his five key papers published at the turn of the last century, mathematically investigated so-called Brownian motion, in which random thermal perturbations in a liquid are responsible for a random walk of randomly arranged particles. His work on a partial differential equation describing motion, the diffusion equation (see Einstein (1905) for his paper in German; English translations were collected and edited by Furth (1926)), tied up an important loose end in the mathematics of transport theory. Einstein's seminal paper provided a firm stochastic, kinetic basis for observations by botanist Robert Brown (1773–1858) and physiologist Jan Ingenhousz (1730–1799) on the random motion of small particles, and

the linear model of Adolf Eugen Fick (1829–1901) describing diffusion in a homogeneous medium. One cannot overstate the convenience and broad applicability of use of partial differential equations, as opposed to one-by-one tracking of motions of particles. Both analytical and numerical formulations for problems ranging from wave phenomena to diffusion to heat conduction in homogeneous media have been used successfully in all branches of science and engineering (table 1). Solutions have also been widely obtained for heterogeneous media, or equivalently, in the case of a class of engineered materials, ‘composite’ media, using both analytical and numerical means (reviewed by Wang & Sastry (2004)).

Software packages are available for solving the diffusion equation within biological cells (see, for example, Schaff *et al.* 1997; Fink *et al.* 2000). There is also an attendant body of literature on the well-posedness of field solutions in the presence of jumps or discontinuities in concentrations of an ionic species (Choi *et al.* 1999). Approaches using ‘cellular automata’ schemes, which involve mimicry of biological behaviours in a regularly parsed domain using simple rules of interaction of elements (Bandini *et al.* 2001; Bandini & Mauri 1999; Weimar 2001; Zanette 1992) have also been used to map intracellular motions. These stem from work by John von Neumann in the 1950s (summarized in von Neumann (1966); for a brief review of scholarly work propagating from this influential effort, see Bandini *et al.* (2001)). These approaches can be extremely efficient in predicting complex behaviour (see, for example, Wolfram 2002). A great deal of effort has been spent in enlarging domains analysed in this fashion, refining solutions and adapting codes to new devices (reviewed by Worsch (1996)). But it remains difficult to tease out the origins of the produced complexity in a physical problem.

Indeed, the tangled filaments of the cytoskeleton are something of a Rorschach test to the modeller: one might see an averaged medium, wherein details of the structures might reasonably be ignored, or, alternatively, a complex domain wherein the local geometry of the network must be taken into account. Though traditional approaches and their solutions have been extremely useful in cell physiology, the next step in understanding ionic transport is not simply characterization, but prediction of ion binding in the dynamic, stochastic, cellular environment. In doing so, there is a potential to grasp the next grail in cellular biochemistry: the satisfactory characterization, and manipulation, of the interplay of key ionic carriers in the cell, and the complete understanding of biometallic homeostasis. It has been recently estimated that there may only be a single free zinc ion in the cell available for binding at any given time (Outten & O’Halloran 2001). Thus, the individual fates of ions may not just be important: in fact, advancement in understanding the relationship between ions and their carriers in signalling functions may hinge on the ability to determine the trajectory of a single ion in the cell.

#### (b) *Key signalling ions and their detection in the cell*

Ionic concentrations in the cell under various physiological and disease states have been assayed for a wide variety of cells. This in turn has led to various hypotheses concerning the origins of fluxes in the cell. In cases of relatively high intracellular concentrations, these formulations have included ‘pumps’ or ‘channels’ which hypothetically drive exchanges of large numbers of ions between cells and their environments. In cases of low overall free-ion concentrations, including intracellular zinc,

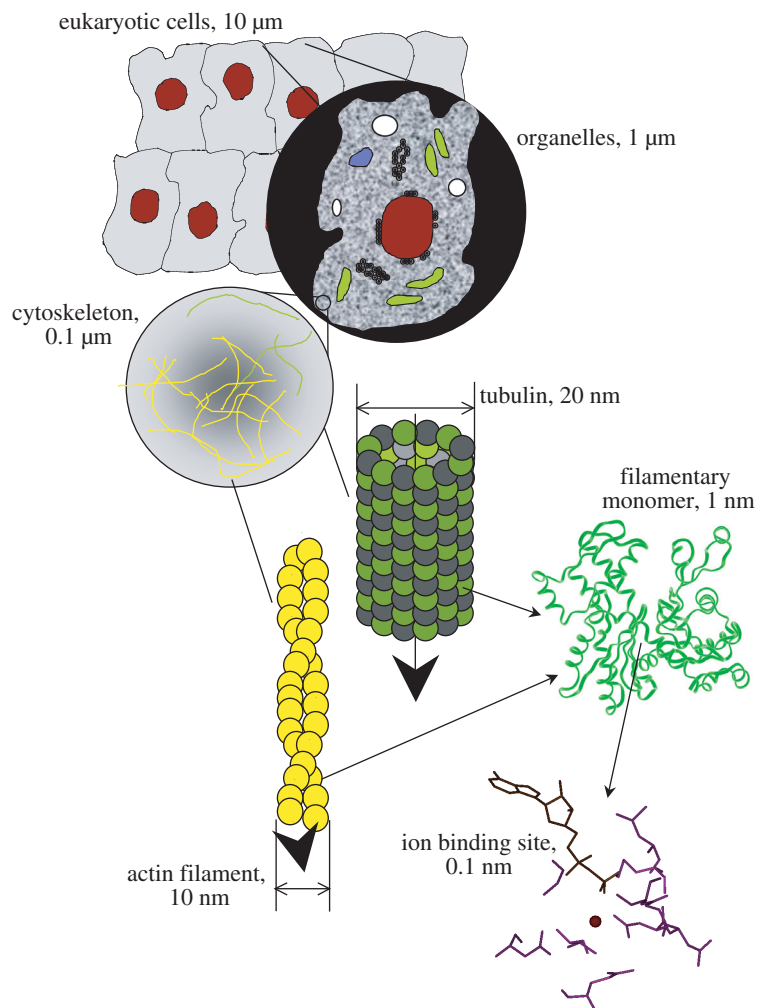


Figure 1. Features of a typical mammalian cell, and their order-of-magnitude sizes, including components of the cytoskeleton associated with material transport. Microtubules (green) convey macromolecules from the nuclear region to the peripheral regions of the cell. Actin filaments (yellow) are cross-linked into a contiguous network for the transport of small ligands and solutes in the outer regions of the cell.

and tightly regulated toxic ionic species, ‘chaperon’ proteins have been postulated to regulate ionic motion.

(i) *Calcium, potassium and sodium*

Sodium and potassium exchange establishes the transmembrane potential across the cell, the gradient responsible for excitability of nerve and muscle cells. Export of sodium from the cell drives the import of glucose, amino acids and other nutrients into the cell. Calcium is another crucial signaller that mediates many biomolecular responses. The intracellular concentrations of potassium and sodium inside a typical

mammalian cell are 140 mM and 5–15 mM, respectively (Pollack 2001). These numbers are reversed for the extracellular concentrations, which are typically 5 mM for potassium and 145 mM for sodium.

(ii) *Zinc*

Biological zinc ( $\text{Zn}^{2+}$ ), an essential trace element for living organisms, is the second most abundant transition metal in seawater and humans, after iron. Zinc ions are involved in diverse biological processes in eukaryotes (Vallee & Falchuk 1993; Berg & Shi 1996). Even moderate zinc deficiency can cause anemia, loss of appetite, immune system defects, developmental problems and teratogenesis (Wood 2000; Hambidge 2000; Takeda 2001). Release of zinc is postulated to promote a synaptic connection and/or modulate post-synaptic receptors and may play an important role in long-term potentiation and learning (Vasak & Hasler 2000). However, uncontrolled zinc release may also cause or accompany neurotoxicity. Prominent pathological effects include acceleration of plaque deposition in Alzheimer's disease and exacerbation of neuron injury that occurs after ischemia, hemorrhage, seizures or mechanical brain trauma (Weiss & Sensi 2000; Bush 2000; Frederickson & Ashley 2001). Figure 2a (adapted from Gaither & Eide (2001)) shows schematically some of the knowns and unknowns about zinc binding and the location of zinc in a cell (*Saccharomyces cerevisiae*). Measurement of the concentration of the rapidly exchangeable intracellular zinc pool remains extremely challenging, due to the low concentrations of  $\text{Zn}^{2+}$  in the presence of high concentrations of other ions such as  $\text{Ca}^{2+}$  and  $\text{Mg}^{2+}$ .

(iii) *Copper*

The trace metal copper ( $\text{Cu}^{2+}$ ) is essential for life as a critical co-factor for enzymes that play key roles in respiration, connective tissue maturation, iron mobilization, protection from free radicals and neuropeptide processing. While copper is an essential element due to its redox chemistry, this same property allows copper to engage in chemical reactions that generate reactive oxygen species capable of damaging DNA, proteins and membranes. In addition to the well-characterized copper-dependent biochemical reactions (figure 2b), changes in copper binding and copper homeostasis have been strongly implicated in Alzheimer's disease, Lou Gehrig's disease (amyotrophic lateral sclerosis) and prion diseases that cause transmissible spongiform encephalopathy. Studies to date demonstrate the existence in virtually all eukaryotic organisms of dedicated and specific high-affinity  $\text{Cu}^{2+}$  transport proteins, denoted Ctr1, at the cell membrane. While Ctr1 serves to move  $\text{Cu}^{2+}$  from the outside environment to the cellular interior, little is known about the quantities and locations of these intracellular  $\text{Cu}^{2+}$  pools (Puig *et al.* 2002; Puig & Thiele 2002).

(iv) *Nanoprobes and detection of ionic species*

Thus, ionic species range in concentration, location and function; important biometals also 'compete' for available sites on proteins, as discussed presently. Recently, nanoprobes have been developed (Zandonella 2003) that pave the way to computational simulation of ion motion and action in the cell. PEBBLE (Probes Encapsulated By Biologically Localized Embedding) sensors may be the smallest of these; spherical sensors (wireless and fibreless) with radii as small as 10 nm have

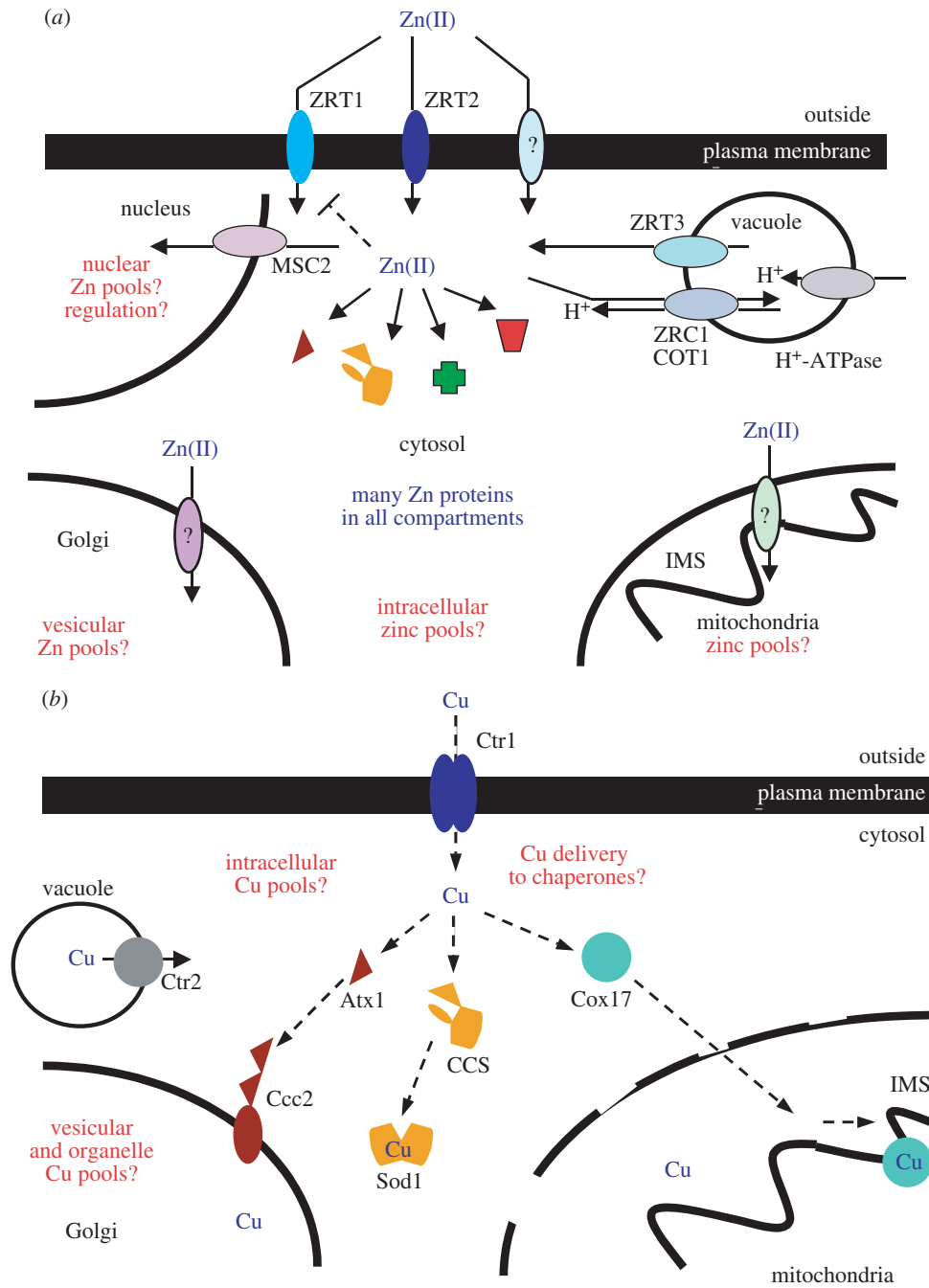


Figure 2. (a) Model of Zn<sup>2+</sup> transport in *S. cerevisiae*. (Image courtesy of Dr Carol A. Fierke, University of Michigan, Ann Arbor, MI). (b) Model for Cu<sup>2+</sup> acquisition and distribution in eukaryotic cells. (Image courtesy of Dr Dennis J. Thiele, Duke University, Durham, NC.)

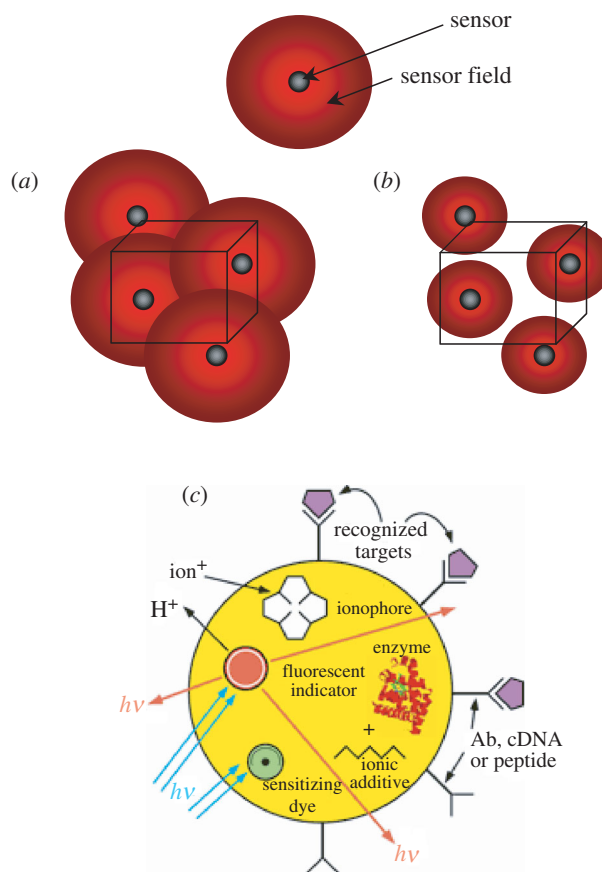


Figure 3. Percolation modelling as a tool in the design of sensor arrays. The density and target affinity of the sensors determines whether detection coverage is (a) complete or (b) incomplete. (c) PEBBLEs, ratiometric sensors for intracellular ions. (Image courtesy of Dr Raoul Kopelman, University of Michigan, Ann Arbor, MI.)

been produced (Brasuel *et al.* 2002; Clark *et al.* 1998, 1999). These probes can be delivered to the cell by a number of techniques, including via gene gun or liposomes. They can also be made ratiometric: sensors can be loaded with two or more fluorescent dyes, one whose emission is invariant to the analyte, and one or more which are dependent upon analyte concentration. In this way, the percentage of sensors that detect analyte can be directly observed: an important issue when the precise number of delivered sensors is difficult to control, due to their size.

Figure 3*a, b* shows two scenarios for systems of intracellular sensors, e.g. PEBBLE sensors (figure 3*c*), having spherical fields. The overall densities, along with the cluster properties, of these sensors determine their collective sensitivity to an analyte. And in the cell, wherein we would like to be able to sense a single ion using a protein that binds it, we have some additional complications. First, for some types of signalling phenomena, dispersion of ions is highly inhomogeneous and non-random. The cytoskeleton itself probably plays a strong role in the transport and storage of ions. Also, the probes are in competition with other binding species, and a mathematical

description of the relative affinities for ionic species of both probes and other transporters or storage vesicles is required in order to model ion exchange. Presently, the classical characterization of ionic concentration is a steady-state, equilibrium measure, namely, affinity (reported as a molarity). This single descriptor in some sense belies the complexity of the dynamic exchange of ions in the cell, in which delivered probes must compete in order to find their targets. Finally, the assumption of a spherical sensor field is a major simplification: proteins have highly specific sites for binding, and their geometric complexity (figure 4) poses challenging energetic and trigonometric calculations to determine site availability for various ions. Mathematically, the statistical effects of sensor shape must be addressed for these complex ‘competitors’ for ions in the cell.

Use of nanotechnologies thus requires a lockstep computational capability: in order to determine the significance of a fluorescence intensity in a ratiometric, optical nanoprobe, experimentally observed intensities must be compared with putative intensities resulting from directed or diffusive transport in the cell. To wit: high relative signal intensity may mark high concentration of the ionic target, or simply reflect high mobility of a relatively low-concentration ionic species, such that probe-ion binding is complete on a timescale much shorter than that of the observation. And the method of transport, along with the complexity of the cellular landscape, makes this a formidable statistical problem indeed. Also, it is important to note that the very presence of a nanoprobe may disrupt the phenomena being observed, and so a mathematical characterization of binding is required that accounts for the actions of both probes and other species that bind ions.

### (c) *Intracellular highways and byways*

The locations and sizes of pools of ions, the proteins that take them there, and the signals they transmit and transduce, are largely prescribed by the internal ‘civil structure’ of the cell. The cytoskeleton physically supports the cell and contains larger vessels which snake through the cytosol, and act as fast routes of transport for macromolecules in addition to streaming ions. Three principal classes of self-assembling polymers comprise the cytoskeleton: actin filaments, microtubules and intermediate filaments.

The first two polymer types have a strong polarity: the monomer units from which the polymers are assembled are asymmetric, but identically aligned so that the filaments have an inherent directionality. Because of their directional nature, actin filaments and microtubules facilitate the transport of solutes and vesicles in prescribed regions of the cytosol. Filamentous actin, or F-actin, is formed by self-assembly of globular or G-actin monomers (Oosawa 2000). A variety of actin-binding proteins bundle and cross-link F-actin into a network of interconnected filaments near the plasma membrane (de la Cruz 2000; Jamney *et al.* 2000). Microtubules are formed within an organizing centre near the cell nucleus, and radiate outward toward the periphery of the cell, forming hollow tubes of diameter 20–24 nm that serve as the tracks for kinesin-based transport of large molecules (e.g. glycoproteins, enzymes), vesicles, and even whole organelles (Brady & Lasek 1982). Intermediate filaments, the third class of cytoskeletal polymers, are 10 nm diameter filaments formed from keratin, nestin and other nondirectional monomer units, and provide mechanical stability to the cell.



Intracellular transport in the cytoplasm likely occurs not only by molecular diffusion, but also by vectorial propagation of ions along networks of actin filaments. Streaming bundles of actin filaments have been observed to undulate conspicuously with propagation rates approaching  $10 \mu\text{m s}^{-1}$  (Pollack 2001). These undulations, which are initiated by complexation of actin with myosin (Sellers 1999), are speculated to induce disordering of the vicinal water that surrounds the filament, with reordering of water in the wake of the undulation. A propagating wavefront of unstructured water, sandwiched between two neighbouring regions of highly ordered water, may act to translate solutes with its volume (Kamitsubo 1972; Szent-Gyorgyi 1972), in a manner analogous to the zone-refining technique used to remove impurities from metal alloys (Pollack 2001). Thus, the rapid propagation of phase transitions within actin filaments suggests that solutes, including metal ions, in the vicinity of the filaments may likewise be entrained in the propagating wave and translated along the filament axis at comparable rates. In this way, filamentary proteins serve a dual role in ionic homeostasis: a site-dense storage area, and also a means of fast transport.

## 2. Transport and sensing: application of percolation concepts to mapping the structure of the cytosol and detection of intracellular ionic motion

### (a) *Debunking diffusion as a key mechanism for intracellular transport*

Returning to our Rorschach test of a micrograph of a complex domain, and armed with an understanding of the highly variable rates of transport observed along and within intracellular filaments and tubules, we see that the structure and the properties of the cytosol defy its characterization as a homogeneous medium for transport. The highly structured membranes within the cell enclose  $100\text{--}200 \text{mm}^3$  of volume and present  $106 \text{mm}^2$  of interfacial surface area per  $1000 \text{mm}^3$  of cytoplasm (Agutter *et al.* (1995), following work by Gershon *et al.* (1983) and Peters (1930)). This structural complexity argues for replacement, where possible, of diffusion modelling with simulation of individual ions, atoms and molecules. Actin has a high negative charge density, so it strongly and non-specifically binds low-molecular-weight solutes (Sheterline *et al.* 1998). Moreover, the regular spacing of charge along the actin filament imposes a high degree of ordering on vicinal water, a condition that is entropically favourable to solute adsorption (Ito *et al.* 1992).

Recently, well-considered critiques of diffusion have appeared, based on known transport mechanisms (see, for example, Agutter *et al.* 1995; Wheatley 2003; Bloom & Goldstein 1998), though direct simulations of intracellular ionic transport with multiple species, at any meaningful timescale, have not yet been reported.

### (b) *Statistical characterization of structure: percolation concepts and transport*

‘Meshing’ techniques have been demonstrated that can map cells using splines, polynomial equations of lines which traverse a complex volume. Stained confocal microscope images have now been used in rendering such three-dimensional (3D) maps. In figure 5 (image and technique following Yi *et al.* (2004)), 200 confocal microscope images of a neuron, each of thickness  $0.1 \mu\text{m}$ , were analysed. Estimates of average sizes and overall density of mitochondria were made, based on the intensity

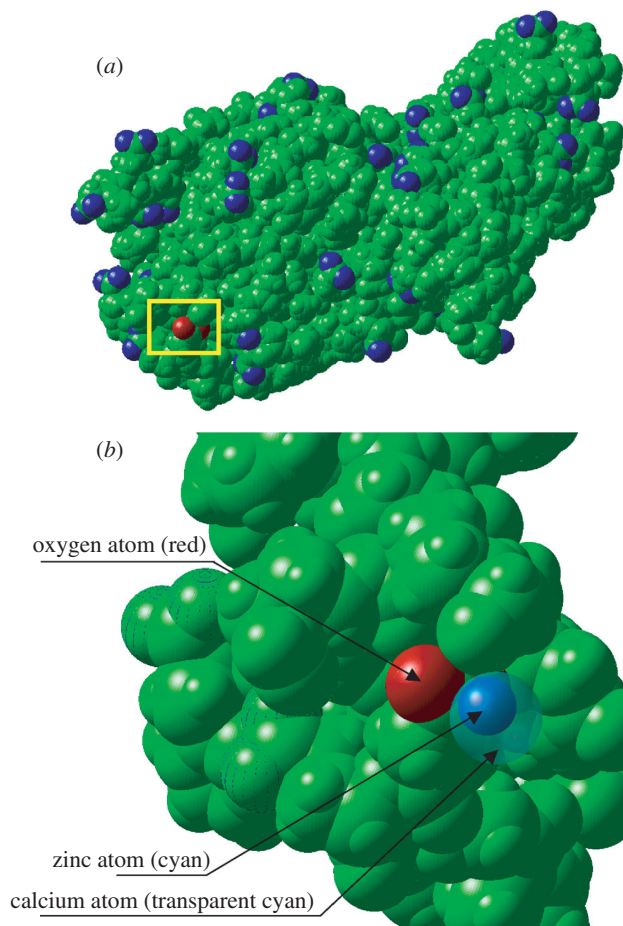


Figure 4. Rendering of the actin monomer, and some results of calculations of site availability for two ions, zinc and calcium (after Shi *et al.* (2004)). In (a), the structure of the monomer is rendered. Atoms are shown as spheres; blue spheres represent negatively charged oxygen atoms that are likely binding sites for either zinc or calcium. Trigonometric calculations (b) in the yellow region indicated by the rectangle in (a) show a possible site that is sterically available to the smaller zinc ion, but not the calcium ion, the latter of which interferes with neighbouring atoms. Both energetic and trigonometric calculations are used to determine site availability. Images were constructed from molecular dynamics simulation using Protein Data Bank structures 1J6Z (Otterbein *et al.* 2001) and 1ATN (Kabsch *et al.* 1990).

of the red dye. Using distribution functions estimated from a few such organelles, this general approach could be used to develop a numerical model for internal organelles. Undoubtedly, the statistical approach in modelling organelles can only be made in the context of the timescale of reorganization of the intracellular features of interest. Here, we have shown mitochondrial clusters, which reorganize on a relatively short timescale as compared with the ionic motions we would like to simulate; other organelles, such as the endoplasmic reticulum, or its cousin in muscle, the sarcoplasmic reticulum, reorganize much more rapidly, and thus alterations in their geometry would have to be simulated in lockstep with protein motion in the cell.

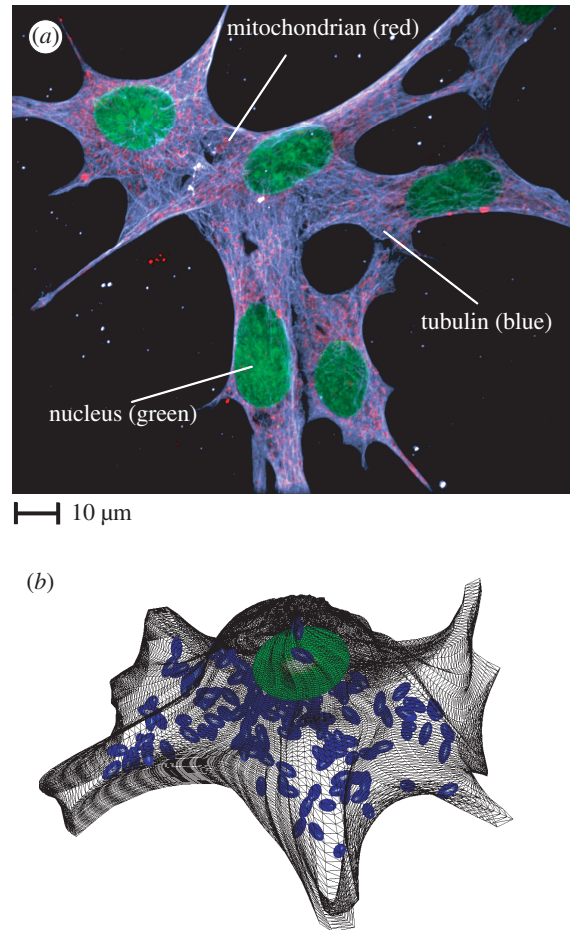


Figure 5. (a) Stained cluster of rat neurons. Nuclei are stained with SYTOX Green; the mitochondria with MitoTracker Red; the tubulin with Anti-b-Tubulin. The smallest analysable feature (a single pixel in the images) is *ca.*  $0.1\ \mu\text{m}$  in diameter. (Image reproduced courtesy of Dr Martin A. Philbert, University of Michigan, Ann Arbor, MI.) (b) Rendering of a 3D model of a neuron shown in (a). 200 confocal images, each of thickness  $0.1\ \mu\text{m}$  were used to develop the model.

We would also like to statistically capture the finer intracellular structures. As shown in figure 1, individual strands of tubulin measure *ca.*  $20\ \text{nm}$  in diameter, and thus they appear in figure 4 as rather cloud-like, and certainly not resolvable with any confidence. However, the individual geometry of tubulin filaments and the overall density of tubulin are known. Understanding, in a statistical sense, the effect of arrangement of these highways is critical to understanding the flow of material, since they are a major contributor to fast transport in the cell.

Models developed for paper (a porous construct of intertwined cellulose fibres), interestingly, were the first to assess clustering and statistical geometry of filamentary structures. Classic work on the crossing densities in systems of lines (Kallmes & Corte 1960) was followed by more detailed modelling of so-called ‘percolation’ thresholds. The concept of percolation is familiar to coffee-drinkers: water ‘percolates’ through

coffee grounds, as it finds multiple paths for flow through the domain, or filter. With a little imagination, we can alter the domain in various ways, and find solutions for a wide variety of transport problems. For example, determination of the minimum number of conductive elements that one must mix into an insulating medium, in order to achieve reasonable conductivity, comprises a percolation problem (Cheng *et al.* 1999; Wang *et al.* 1999, 2000; Wang & Sastry 2000). Determination of a critical number of stiff, randomly arrayed nanotubes necessary to achieve reasonable stiffness in the porous material is another (Berhan *et al.* 2004). In fact, statistical geometry can be used to obtain percolation solutions in virtually any medium (even air) randomly infused with a second, possibly percolating phase, using numerical or sometimes even analytical approaches, so long as the geometry of the particles of interest is known.

Work in paper was recently extended to fibres of varying degrees of waviness, as intracellular filaments exemplify (Yi & Sastry 2004). Using molecular dynamics simulations, we are nearly at the point of combining models for ionic motion with those of statistical geometry to yield realistic transport rates. But in addition to describing geometry statistically, with an eye to determining the significant densities of features, and the characteristic distances that species are transported along those features, percolation concepts have another very useful function in facilitating the design of sensor arrays.

*(c) Sensing events in a complex domain:  
percolation concepts and design of sensor arrays*

We demonstrate a general approach in cluster statistics, using a simple but classical example. Suppose we denote as  $p$  the probability that a bond connects two points on a square grid, and as  $q$ , the probability that a bond is absent. If points can only be connected in the  $x$ - and  $y$ -directions, there are exactly two configurations for which a cluster of bonds of size two can arise, as shown in figure 6. The probability,  $P_2$ , that a bond is a member of a cluster of size two is simply the sum of the probabilities of either case, namely

$$P_2 = 2p^2q^8 + 4p^2q^8 = 6p^2q^8 = 6p^2(1-p)^8. \quad (2.1)$$

Now suppose that we are interested in systems that are not conveniently described as falling on a Cartesian grid, but instead contain clusters of particles that overlap. We must define, mathematically, a few terms to describe the cluster properties. First, we define the ‘cluster number’,  $n_k$ , as the ratio of the number of clusters of size  $k$ , to the total number of particles. The ‘mean cluster size’ is defined as

$$S = \sum_{k=1}^{\infty} k^2 n_k. \quad (2.2)$$

We can use this cluster size to predict the percolation status in any system: when the mean cluster size becomes unbounded, we have achieved percolation in the system, since there exists at least one infinite cluster that must span the domain.

As discussed previously, the sensing field, rather than being simply spherical, is irregular in shape. As a first approximation beyond a spherical field, we might transcribe an ellipsoid around the protein to represent the sensed volume, accounting for

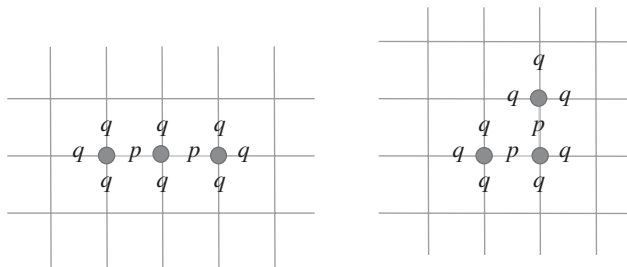


Figure 6. Sketch of the two possible configurations of clusters of two segments on a square grid. Values  $p$  and  $q$  are the probabilities of existence and absence of a bond, respectively.

its various sites and affinities. An integral approach extending analytical solutions for percolation thresholds was recently obtained for both two-dimensional (2D) systems of ellipses (Yi & Sastry 2002) and 3D systems of ellipsoids (Yi & Sastry 2004). Thus, analytical solutions have now been developed to predict percolation onset in systems of non-circular and non-spherical particles, along with attendant solutions for probabilities of cluster sizes arising in all of these systems. Such an integral technique could also be expanded to other geometries, though for very complex systems direct simulation may be required.

### 3. Simulation of the competition for ions in the cell: the future of multiscale modelling

To apply percolation concepts to the sensing of cytosolic ions, a key piece of information is needed: the distance over which each sensor can detect ions. The size and shape of the detection field around each sensor necessarily depend on the rate at which unbound ions propagate within the cytoplasm. Molecular dynamics (MD) simulations can be used to determine the transport characteristics of these complex heterogeneous systems. Thermodynamic and transport properties are determined from configuration sampling of the protein–ion–solvent system at the atomic level, using a force field that is a summation of the covalent bond energies and non-bonded interactions (e.g. Coulombic charge attraction/repulsion; dispersion forces; hydrogen bonding) to generate atomic coordinates at successive time-steps. MD simulations of biological macromolecules thus require both a suitable parametrized force field, e.g. CHARMM (Brooks *et al.* 1983), and knowledge of the three-dimensional structure of the protein.

With the processor speeds and load-distribution capabilities of state-of-the-art computing clusters, MD simulations of solvated proteins are now possible. Much of the biomolecule simulation activity has been directed toward studies of ion permeation through outer membrane channel proteins (Tieleman *et al.* 2001), but more recently molecular simulations of actin have been carried out to investigate its polymerization (Sept *et al.* 1999) and its complexation with actin binding proteins (Wriggers *et al.* 1998).

The structures of the actin and tubulin monomers have been solved from X-ray diffraction crystallography, and the coordinates of these structures reposted in the Protein Data Bank (<http://www.rcsb.org/pdb>) may be used to generate model filament structures to determine the binding sites for metal ions on the filament; the

effect of competition among ions for a select number of filament binding sites; and the rate constants for association/dissociation and streaming of ions along the filaments.

MD simulations of the actin monomer (Shi *et al.* 2004) show that the five sites that most strongly adsorb  $\text{Ca}^{2+}$  on the monomer are identical to five of the six crystallographically resolved  $\text{Ca}^{2+}$  sites. In the cell, however, other ions besides calcium compete for these sites, just as various proteins compete for specific ions; one imagines an ionic shoving match along the filaments of the cell, particularly among abundant species. As with any physical contest, both size and numbers matter. In the contest between  $\text{Mg}^{2+}$  and  $\text{Ca}^{2+}$ , the high cytosolic ratio of magnesium to calcium (5000:1) gives  $\text{Mg}^{2+}$  a strong advantage in occupying the high-affinity sites on physiological actin, even though  $\text{Ca}^{2+}$  has a larger binding energy than  $\text{Mg}^{2+}$  (Strzelecka-Golaszewska *et al.* 1978).

Beyond looking at competition between specific ions for specific sites on a single protein, we need a more general, but still computationally efficient, means of simulating the transport of multiple ions to and from various sites and locations in the cell. The electrical field and mean ion diffusivity calculated around a protein from MD simulation may be used as input parameters to a Brownian dynamics (BD) simulation (Sansom *et al.* 2000) for this task. BD simulation enables statistically meaningful calculation of ion propagation over timescales of microseconds, far exceeding the nanosecond grasp of a conventional MD simulation. A combined MD/BD approach can thus, for example, yield the trajectories of trace biometals such as  $\text{Zn}^{2+}$  or  $\text{Cu}^{2+}$  as the ions hopscotch along actin filaments from one weak affinity site ( $10^{-2}$  M) to the next. The trajectories are almost certainly species dependent, as experimental evidence indicates, for example, that the affinity binding sites for  $\text{Zn}^{2+}$  on actin are distinct from those of  $\text{Ca}^{2+}$  and  $\text{Mg}^{2+}$  (Strzelecka-Golaszewska 1973). The ion propagation rates and trajectories extracted from molecular-level simulation thus inform the percolation model of the sensor array constructed at the cell-spanning level in the multiscale hierarchy, by assigning a physiologically valid detection radius to each sensor.

Finally, so-called Monte Carlo simulations are required. Once the energetics and site availability are known, one must still simulate the dynamic exchange of ions. And in physics, as in life, initial conditions are everything. To realistically predict the winners in the competition for ions, millions of scenarios of starting conditions for the numbers, strengths and locations of ‘binders’ (the term here generically applies to both probes and native proteins in the cell, including low-affinity ion ‘storage’ proteins) must be considered in order to determine probable outcomes. Clearly, these first computational experiments must be run for model systems, since our present understanding of cellular ion transporters is incomplete in both prokaryotes and eukaryotes. But the scientific community is tantalizingly close to achieving the direct comparisons needed between experiment and theory to validate models of intracellular transport (with steps outlined in figure 7). Modern imaging of 3D cell structure will feed directly into the statistical models needed for characterization, and atomistic simulations will ultimately provide sufficient information on pairwise ion–protein interactions to move on to complex interactions between multiple ions and proteins. Identification of transporter proteins, determination of binding sites on cytoskeletal structures, and large-scale simulations of competition between the proteins that participate in ion homeostasis will undoubtedly form the basis for the major results in biochemistry in the coming years. As with genomics, intensive

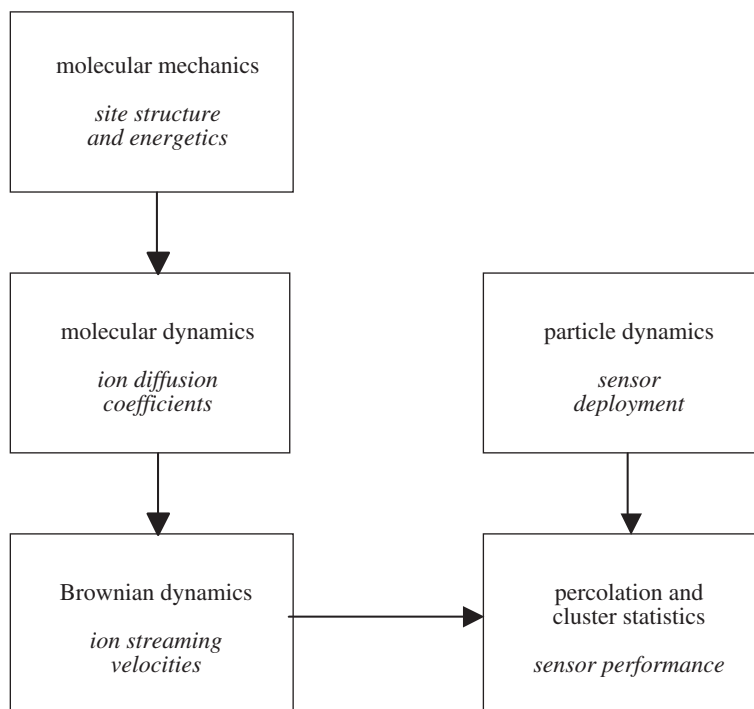


Figure 7. Likely path of hierarchical simulation approaches to modelling intracellular binding events.

collaboration among computational scientists, biochemists, physiologists and other specialists will be required for breakthroughs.

We first and foremost thank the students and research associates with whom we have had the pleasure of working. We acknowledge insights provided by our collaborators, Dr Carol Fierke, Dr Raoul Kopelman, Dr Martin Philbert and Dr Dennis Thiele. We especially acknowledge the contributions of Dr Yun-Bo Yi, Dr Chia-Wei Wang, Dr Wei Shi and Mr Munish Inamdar. We would also like to acknowledge the inspiration provided by our favourite collaborations, our children, Katie and Peter Lastoskie, who are the joy of our lives.

Funding for this work was provided by the W. M. Keck Foundation, and the US National Science Foundation. Modelling work was performed on a Sun Fire computing cluster, a gift of Sun Microsystems to the authors. We appreciate the generous support of our sponsors.

## References

- Agutter, P. S., Malone, P. C. & Wheatley, D. N. 1995 Intracellular transport mechanisms: a critique of diffusion theory. *J. Theor. Biol.* **176**, 261–272.
- Bandini, S. & Mauri, G. 1999 Multilayered cellular automata. *Theor. Comp. Sci.* **217**, 99–113.
- Bandini, S., Mauri, G. & Serra, R. 2001 Cellular automata: from a theoretical parallel computation model to its application to complex systems. *Par. Comput.* **27**, 539–553.
- Berg, J. M. & Shi, Y. 1996 The galvanization of biology: a growing appreciation for the roles of zinc. *Science* **271**, 1081–1085.
- Berhan, L., Yi, Y.-B. & Sastry, A. M. 2004 Effect of nanorope waviness on the effective moduli of nanotube sheets. *J. Appl. Phys.* **95**(9), 5027–5034.

- Bloom, G. S. & Goldstein, L. S. B. 1998 Cruising along microtubule highways: how membranes move through the secretory pathway. *J. Cell. Biol.* **140**, 1277–1280.
- Bootman, M. D., Berridge, M. J. & Lipp, P. 1997 Cooking with calcium: the recipes for composing global signals from elementary events. *Cell* **91**, 367–373.
- Brady, S. & Lasek, R. 1982 *Meth. Cell Biol.* **25**, 365.
- Brasuel, M., Aylott, J. W., Clark, H., Xu, H., Kopelman, R., Hoyer, M., Miller, T. J., Tjalkens, R. & Philbert, M. A. 2002 Production, characteristics and applications of fluorescent PEBBLE nanosensors: potassium, oxygen, calcium and pH imaging inside live cells. *Sensors Mater.* **6**, 1–29.
- Brooks, B. R., Bruccoleri, R. E., Olafson, B. D., States, D. J., Swaminathan, S. & Karplus, M. 1983 CHARMM: a program for macromolecular energy, minimization, and dynamics calculations. *J. Computat. Chem.* **4**, 187–217.
- Bush, A. I. 2000 Metals and neuroscience. *Curr. Opin. Chem. Biol.* **4**, 184–191.
- Cheng, X., Wang, C. W., Sastry, A. M. & Choi, S. B. 1999, Investigation of failure processes in porous battery substrates. II. Simulation results and comparisons. *ASME J. Engng Mater. Technol.* **121**, 514–523.
- Choi, Y. S., Resasco, D., Schaff, J. & Slepchenko, B. 1999 Electrodiffusion of ions inside living cells. *IMA J. Appl. Math.* **62**, 207–226.
- Clark, H. A., Barker, S. L. R., Kopelman, R., Hoyer, M. & Philbert, M. A. 1998 Subcellular optochemical nanobiosensors: probes encapsulated by biologically localized embedding (PEBBLEs). *Sens. Actuators B* **51**, 12–16.
- Clark, H. A., Hoyer, M., Philbert, M. A. & Kopelman, R. 1999 Optical nanosensors for chemical analysis inside single living cells. 1. Fabrication, characterization, and methods for intracellular delivery of PEBBLE sensors. *Analyt. Chem.* **71**, 4831–4836.
- de la Cruz, E. M. 2000 Actin-binding proteins: an overview. In *Molecular interactions of actin* (ed. C. G. dos Remedios & D. D. Thomas), pp. 122–134. Springer.
- Einstein, A. 1905 Über die von der molekularkinetischen Theorie der warme geforderte Bewegung von in ruhenden Flüssigkeiten suspendierten Teilchen. *Annln Phys.* **17**, 549–560.
- Fink, C. C., Slepchenko, B., Moraru, I. I., Watras, J., Schaff, J. & Loew, L. M. 2000 An image-based model of calcium waves in differentiated neuroblastoma cells. *Biophys. J.* **79**, 163–183.
- Frederickson, J. C. & Ashley, I. B. 2001 Synaptically released zinc: physiological functions and pathological effects. *BioMetals* **14**, 353–366.
- Furth, R. (ed.) 1926 *Investigations on the theory of the Brownian movement* (by Albert Einstein, transl. A. D. Cowper). New York: E. P. Dutton & Co.
- Gaither, L. A. & Eide, D. J. 2001 Eukaryotic zinc transporters and their regulation. *BioMetals* **14**, 252–270.
- Gershon, N., Porter, K. & Trus, B. 1983 The microtravecular lattice and the cytoskeleton: their volume, surface area and the diffusion of molecules through them. In *Biological structures and coupled flows* (ed. A. Oplatka & M. Balaban), pp. 377–380. New York: Academic.
- Hambidge, M. 2000 Human zinc deficiency. *J. Nutrition* **130**, 1344S–1349S.
- Ito, T., Suzuki, A. & Stossel, T. P. 1992 Regulation of water flow by actin-binding protein-induced actin gelation. *Biophys. J.* **61**, 1301–1305.
- Jamney, P. A., Shah, J. V., Tang, J. X. & Stossel, T. P. 2000 Actin filament networks. In *Molecular interactions of actin* (ed. C. G. dos Remedios & D. D. Thomas), pp. 181–199. Springer.
- Kabsch, W., Mannherz, H. G., Suck, D., Pai, E. F. & Holmes, K. C. 1990 Atomic structure of the actin:DNase I complex. *Nature* **347**, 37–44.
- Kallmes, O. & Corte, H. 1960 The statistical geometry of an ideal two dimensional fiber network. *TAPPI J.* **43**, 737–752.
- Kamitsubo, E. 1972 Motile protoplasmic fibrils in cells of the characeae. *Protoplasma* **74**, 53–70.



- Oosawa, F. 2000 A historical perspective of actin assembly and its interactions. *Molecular interactions of actin* (ed. C. G. dos Remedios & D. D. Thomas), pp. 9–21, Springer.
- Otterbein, L. R., Graceffa, P. & Dominguez, R. 2001 The crystal structure of uncomplexed actin in the Adp state. *Science* **293**, 708–711.
- Outten, C. E. & O'Halloran, T. V. 2001 Femtomolar sensitivity of metalloregulatory proteins controlling zinc homeostasis. *Science* **292**, 2488–2492.
- Peters, R. A. 1930 Surface structure in the integration of cell activity. *Trans. Faraday Soc.* **26**, 797–807.
- Pollack, G. H. 2001 *Cells, gels and the engines of life*. Seattle, WA: Ebner and Sons.
- Puig, S. & Thiele, D. J. 2002 Molecular mechanisms of copper uptake and distribution. *Curr. Opin. Chem. Biol.* **6**, 171–180.
- Puig, S., Rees, E. M. & Thiele, D. J. 2002 The ABCDs of periplasmic copper trafficking. *Structure* **10**, 1292–1295.
- Sansom, M. S. P., Shrivastava, I. H., Ranatunga, K. M. & Smith, G. R. 2000 Simulations of ion channels—watching ions and water move. *Trends Biochem. Sci.* **25**, 368–374.
- Schaff, J., Fink, C., Slepchenko, B., Carson, J. & Loew, L. 1997 A general computational framework for modeling cellular structure and function. *Biophys. J.* **73**, 1135–1146.
- Sellers, J. R. 1999 *Myosins* (2nd edn). Oxford University Press.
- Sept, D., Elcock, A. H. & McCammon, J. A. 1999 Computer simulations of actin polymerization can explain the barbed-pointed end asymmetry. *J. Mol. Biol.* **294**, 1181–1189.
- Sheterline, P., Clayton, J. & Sparrow, J. C. 1998 *Actin* (4th edn). Oxford University Press.
- Shi, W., Inamdar, M., Sastry, A. M. & Lastoskie, C. M. 2004 Energetics and accessibility of divalent cation adsorption on the actin monomer. (Submitted.)
- Strzelecka-Golaszewska, H. 1973 Relative affinities of divalent cations to the site of the tight calcium binding in g-actin. *Biochim. Biophys. Acta* **370**, 60–69.
- Strzelecka-Golaszewska, H., Prochniewicz, E. & Drabikowski, W. 1978 Interaction of actin with divalent cations. 1. The effect of various cations on the physical state of actin. *Eur. J. Biochem.* **88**, 219–227.
- Szent-Gyorgyi, A. 1972 *The living state, with observations on cancer*. Academic.
- Takeda, A. 2001 Zinc homeostasis and functions of zinc in the brain. *BioMetals* **14**, 343–351.
- Tieleman, D. P., Biggin, P. C., Smith, G. R. & Sansom, M. S. P. 2001 Simulation approaches to ion channel structure–function relationships. *Q. Rev. Biophys.* **34**, 473–561.
- Vallee, B. L. & Falchuk, K. H. 1993 The biochemical basis of zinc physiology. *Physiol. Rev.* **73**, 79–118.
- Vasak, M. & Hasler, D. W. 2000 Metallothioneins: new functional and structural insights. *Curr. Opin. Chem. Biol.* **4**, 177–183.
- von Neumann, J. 1966 *Theory of self-reproducing automata*. University of Illinois Press.
- Wang, C.-W. & Sastry, A. M. 2000 Structure, mechanics and failure of stochastic fibrous networks. II. Network simulation and application. *ASME J. Engng Mater. Technol.* **122**, 460–468.
- Wang, C.-W. & Sastry, A. M. 2004 Composites. In *Encyclopedia of biomaterials and biomedical engineering* (ed. G. E. Wnek & G. L. Bowlin), pp. 355–372. New York: Marcel Dekker.
- Wang, C. W., Cheng, X., Sastry, A. M. & Choi, S. B. 1999 Investigation of failure processes in porous battery substrates. I. Experimental findings. *ASME J. Engng Mater. Technol.* **121**, 03–513.
- Wang, C.-W., Berhan, L. & Sastry, A. M. 2000 Structure, mechanics and failure of stochastic fibrous networks. I. Microscale considerations. *ASME J. Engng Mater. Technol.* **122**, 450–459.
- Weimar, J. R. 2001 Coupling microscopic and macroscopic cellular automata. *Par. Comput.* **27**, 601–611.
- Weiss, J. H. & Sensi, S. L. 2000  $\text{Ca}^{2+}$ – $\text{Zn}^{2+}$  permeable AMPA or kainate receptors: possible key factors in selective neurodegeneration. *Trends Neurosci.* **23**, 365–371.

- Wheatley, D. N. 2003 Diffusion, perfusion and the exclusion principles in the structural and functional organization of the living cell: reappraisal of the properties of the 'ground substance' (review). *J. Exp. Biol.* **206**, 1955–1961.
- Wolfram, S. 2002 *A new kind of science*. Champaign, IL: Wolfram Media.
- Wood, R. J. 2000 Assessment of marginal zinc status in humans. *J. Nutrition* **130**, 1350S–1354S.
- Worsch, T. 1996 Programming environments for cellular automata. In *Proc. ACRI'96* (ed. S. Bandini & G. Mauri), pp. 3–12. Springer.
- Wriggers, W., Tang, J. X., Azuma, T., Marks, P. W. & Janmey, P. A. 1998 Cofilin and gelsolin segment-1: molecular dynamics simulation and biochemical analysis predict a similar actin binding mode. *J. Mol. Biol.* **282**, 921–932.
- Yi, Y. B. & Sastry, A. M. 2002 Analytical approximation of the two-dimensional percolation threshold for fields of overlapping ellipses. *Phys. Rev. E* **66**, 066130.
- Yi, Y. B. & Sastry, A. M. 2004 Analytical approximation of the percolation threshold for overlapping ellipsoids of revolution. *Proc. R. Soc. Lond. A* **460**, 2353–2380.
- Yi, Y.-B., Berhan, L. & Sastry, A. M. 2004 Statistical geometry of random fibrous networks, revisited: waviness, dimensionality and percolation. *J. Appl. Phys.* **96**(3), 1–10.
- Yi, Y.-B., Sastry, A. M. & Philbert, M. A. 2004 Three-dimensional reconstruction of cell boundaries and interior organelles from confocal microscopy, using a combined delaunay tessellation/stochastic placement scheme. (Submitted.)
- Zandonella, C. 2003 Cell nanotechnology: the tiny toolkit. *Nature* **423**, 10–12.
- Zanette, D. H. 1992 Multistate cellular automaton for reaction-diffusion processes. *Phys. Rev. A* **46**, 7573–7577.

## AUTHOR PROFILES

### A. M. Sastry



Ann Marie Sastry was born in and spent her childhood in Illinois. She studied Mechanical Engineering at the University of Delaware, graduating in 1989; she and Christian Lastoskie were married in the same year. She obtained her PhD in Mechanical Engineering at Cornell University in 1993, and then worked as a Research Scientist at Sandia National Laboratories. In 1995, she joined the University of Michigan as an Assistant Professor of Mechanical Engineering and Applied Mechanics. She received the Presidential Early Career Award from the US National Science Foundation in 1997 and the Henry Russell Award from the University of Michigan in 1998. At the age of 36, she is presently an Associate Professor in the Departments of Mechanical Engineering, Materials Science and Engineering and Biomedical Engineering at the University of Michigan. Her scientific interests are in percolation modelling, fibrous network theory and the application of these methods to the study of biological tissues, electrode materials and composite structures.

**C. M. Lastoskie**

A native of Pennsylvania, Christian Lastoskie studied Chemical Engineering at the University of Delaware, graduating in 1989. He completed his PhD in Chemical Engineering at Cornell University in 1994. After appointments as a Research Scientist at Sandia National Laboratories and Visiting Professor at the University of Michigan, he joined Michigan State University in 1996 as an Assistant Professor of Chemical Engineering. He received the Career Award from the US National Science Foundation in 1998 and the Teacher-Scholar Award from Michigan State University in 2000. In 2001, he joined the University of Michigan, where, now aged 37, he is currently an Associate Professor in the Departments of Civil and Environmental Engineering and Biomedical Engineering. His scientific interests are in the atomistic simulation of adsorption and transport in porous materials and biological systems. He and his wife, Ann Marie Sastry, are the parents of Katherine, aged 7, and Peter, aged 3.